

Molecular and Electronic Structure of Five-Coordinate Complexes of Iron(II/III) Containing *o*-Diiminobenzosemiquinonate(1−) π Radical Ligands

Krzysztof Chłopek, Eckhard Bill, Thomas Weyhermüller, and Karl Wieghardt*

Max-Planck-Institut für Bioorganische Chemie, Stiftstrasse 34-36,
D-45470 Mülheim an der Ruhr, Germany

Received May 23, 2005

The reaction of the ligand *N*-phenyl-1,2-benzenediamine (*N*-phenyl-*o*-phenylenediamine), $\text{H}_2[\text{L}^{\text{PDI}}]$, in dry acetonitrile with $[\text{Fe}^{\text{III}}(\text{dmf})_6](\text{ClO}_4)_3$ (dmf = *N,N*-dimethylformamide) affords the dimer (μ -NH,NH) $[\text{Fe}^{\text{III}}(\text{L}^{\text{ISQ}})(\text{L}^{\text{PDI}})]_2$ (**1**), where $(\text{L}^{\text{ISQ}})^{\bullet-}$ represents the π radical monoanion *N*-phenyl-*o*-diiminobenzosemiquinonate and $(\text{L}^{\text{PDI}})^{2-}$ is its one-electron-reduced, closed-shell form. Complex **1** possesses a diamagnetic ground-state $S_t = 0$. Addition reactions of tri-*n*-butylphosphane, *tert*-butyl isocyanide, cyclohexyl isocyanide, 4,5-diphenylimidazole, and 4-(1-phenylpentyl)pyridine with **1** in acetonitrile or toluene yields $[\text{Fe}^{\text{II}}(\text{L}^{\text{ISQ}})_2(\text{PBU}_3)]$ (**2**), $[\text{Fe}^{\text{II}}(\text{L}^{\text{ISQ}})_2(\text{CN}^t\text{Bu})]$ (**4**), $[\text{Fe}^{\text{II}}(\text{L}^{\text{ISQ}})_2(\text{CNCy})]$ (**5**), $[\text{Fe}^{\text{III}}(\text{L}^{\text{ISQ}})_2(\text{Ph}_2\text{Im})]$ (**6**), and $[\text{Fe}^{\text{III}}(\text{L}^{\text{ISQ}})(\text{L}^{\text{PDI}})(\text{BuPhCH-py})]\text{-BuPhCH-py}$ (**7**). Oxidation of **1** with iodine affords $[\text{Fe}^{\text{III}}(\text{L}^{\text{ISQ}})_2]$ (**3**), and oxidation of **2** with ferrocenium hexafluorophosphate yields $[\text{Fe}^{\text{III}}(\text{L}^{\text{ISQ}})_2(\text{PBU}_3)](\text{PF}_6)$ (**2^{ox}**). The structures of complexes **2**, **2^{ox}**, **3**, **5**, **6**, and **7** have been determined by X-ray crystallography at 100(2) K. Magnetic susceptibility measurements and EPR, UV–vis, and Mössbauer spectroscopy have established that mononuclear complexes containing the $[\text{Fe}^{\text{II}}(\text{L}^{\text{ISQ}})_2\text{X}]$ chromophore (**2**, **4**, **5**) are diamagnetic ($S_t = 0$) whereas those with an $[\text{Fe}^{\text{II}}(\text{L}^{\text{ISQ}})_2\text{X}]^n$ chromophore (**3**, **2^{ox}**, **6**) are paramagnetic ($S_t = 1/2$) and those with an $[\text{Fe}^{\text{III}}(\text{L}^{\text{ISQ}})(\text{L}^{\text{PDI}})\text{X}]$ chromophore (**7**) possess an $S_t = 1$ ground state. It is established that all ferric species have an intrinsic intermediate spin ($S_{\text{Fe}} = 3/2$) which is intramolecularly antiferromagnetically coupled to one or two $(\text{L}^{\text{ISQ}})^{\bullet-}$ ligand radicals yielding an $S_t = 1$ (**7**) or $S_t = 1/2$ (**2^{ox}**, **3**, **6**) ground state, respectively. In the ferrous complexes **2**, **4**, and **5** the intrinsic spin at the iron ion is either low spin ($S_{\text{Fe}} = 0$) or intermediate spin ($S_{\text{Fe}} = 1$). Antiferromagnetic coupling between two radicals $(\text{L}^{\text{ISQ}})^{\bullet-}$ or, alternatively, between the intermediate spin ferrous ion and two radicals yields then the observed diamagnetic ground state. In **1** two $[\text{Fe}^{\text{III}}(\text{L}^{\text{ISQ}})(\text{L}^{\text{PDI}})]$ halves with $S^* = 1$ couple antiferromagnetically affording an $S_t = 0$ ground state.

Introduction

It is well established that the doubly deprotonated ligand derived from *o*-phenylenediamine, $\text{H}_2[\text{L}_{\text{N,N}}^{\text{PDI}}]$, can exist in three distinctly different oxidation levels in coordination compounds as (1) the *N,N*-coordinated, closed-shell dianion *o*-phenylenediimide(2−), $(\text{L}_{\text{N,N}}^{\text{PDI}})^{2-}$, (2) its monoanionic π radical *o*-diiminobenzosemiquinonate(1−), $(\text{L}_{\text{N,N}}^{\text{ISQ}})^{\bullet-}$, or (3) the neutral *o*-diiminobenzoquinone, $(\text{L}_{\text{N,N}}^{\text{IBQ}})^0$.^{1,2} These forms possess significantly different C–N and C–C bond distances as shown in Scheme 1. Balch and Holm³ have shown in 1966 that the square planar complexes $[\text{M}(\text{L}_{\text{N,N}}^{\text{ISQ}})_2]$ (M = Ni, Pd,

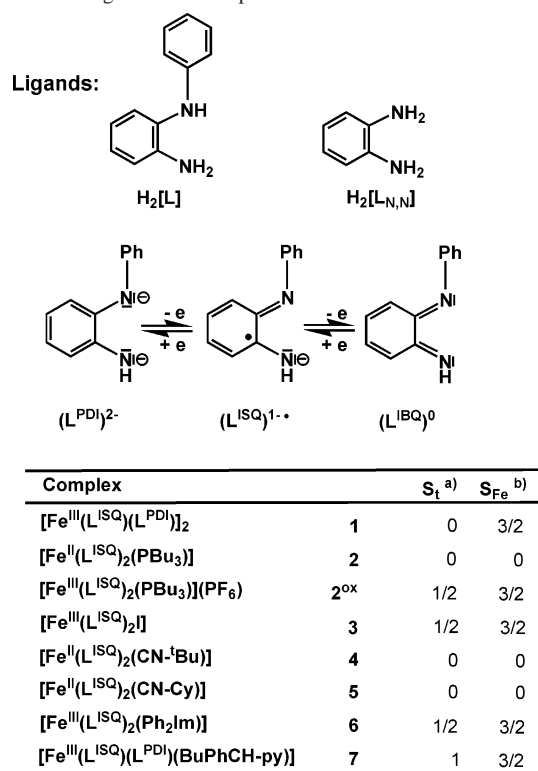
Pt, Co) can be twice reversibly one-electron oxidized and, similarly, twice reduced yielding an electron-transfer series of five square planar species $[\text{ML}_2]^{2+,1+,0,1-,2-}$ each of which contains a divalent metal ion: $[\text{Ni}^{\text{II}}(\text{L}_{\text{N,N}}^{\text{IBQ}})_2]^{2+}$; $\text{Ni}^{\text{II}}(\text{L}_{\text{N,N}}^{\text{ISQ}})(\text{L}_{\text{N,N}}^{\text{IBQ}})]^+$; $[\text{Ni}^{\text{II}}(\text{L}_{\text{N,N}}^{\text{ISQ}})_2]^0$; $[\text{Ni}^{\text{II}}(\text{L}_{\text{N,N}}^{\text{ISQ}})(\text{L}^{\text{PDI}})]^-$; $[\text{Ni}^{\text{II}}(\text{L}_{\text{N,N}}^{\text{PDI}})_2]^{2-}$. We have recently shown that exactly the same analogues are available using the ligand *N*-phenyl-1,2-benzenediamine.^{2,4,5}

In 1977 Warren⁶ reported two interesting iron complexes containing *o*-phenylenediimide derived ligands both of which

(1) (a) Mederos, A.; Dominguez, S.; Hernandez-Molina, R.; Sanchiz, J.; Brito, F. *Coord. Chem. Rev.* **1999**, 193–195, 913. (b) Carugo, O.; Djinovic, K.; Rizzi, M.; Castellani, C. B. *J. Chem. Soc., Dalton Trans.* **1991**, 1551.

* To whom correspondence should be addressed. E-mail: wieghardt@mpi-muelheim.mpg.de.

Scheme 1. Ligands and Complexes



a) Electronic ground state of complex; b) intrinsic spin state of iron ion.

were reported to possess an $S_t = 1/2$ ground state: $[\text{Fe}\{\text{C}_6\text{H}_4(\text{NH})_2\}_2\text{I}]$ (**a**) and $[\text{Fe}\{\text{C}_6\text{H}_4(\text{NH})_2\}_2(\text{PPh}_3)](\text{PF}_6)$ (**b**). The diamagnetic octahedral species $[\text{Fe}^{\text{II}}(\text{L}_{\text{N,N}}^{\text{IBQ}})_3](\text{PF}_6)_2$ ($S_t = 0$) and $[\text{Fe}^{\text{II}}(\text{CN})_4\{\text{C}_6\text{H}_4(\text{NH})_2\}_2]^{2-}$ had also been reported and structurally characterized.^{7,8} The latter two complexes undoubtedly contain a low-spin ferrous ion and neutral, N,N' -coordinated quinonediimine ligands, $(\text{L}_{\text{N,N}}^{\text{IBQ}})$, but the molecular and electronic structures are unclear. Warren⁶ had proposed that **a** and **b** each contain a low-spin ferric ion ($S_{\text{Fe}} = 1/2$) coupled in an antiferromagnetic fashion to two ligand π radicals $(\text{L}_{\text{N,N}}^{\text{ISQ}})^{\cdot-}$. In contrast, in two recent publications we have shown that two similar complexes containing two *o*-iminobenzosemiquinonate(1-), $(\text{L}_{\text{N,O}}^{\text{ISQ}})^{\cdot-}$, and two *o*-iminothionebenzosemiquinonate(1-), $(\text{L}_{\text{N,S}}^{\text{ISQ}})^{\cdot-}$, π radicals, respectively, namely $[\text{Fe}^{\text{III}}(\text{L}_{\text{N,O}}^{\text{ISQ}})_2\text{I}]$ and $[\text{Fe}^{\text{III}}(\text{L}_{\text{N,S}}^{\text{ISQ}})_2\text{I}]$, contain an *intermediate*-spin ferric ion ($S_{\text{Fe}} = 3/2$) antiferromagnetically coupled to the two ligand radicals yielding an $S_t = 1/2$ ground state.^{9,10}

- (2) (a) Herebian, D.; Bothe, E.; Neese, F.; Weyhermüller, T.; Wieghardt, K. *J. Am. Chem. Soc.* **2003**, *125*, 9116 and references therein. (b) Herebian, D.; Wieghardt, K.; Neese, F. *J. Am. Chem. Soc.* **2003**, *125*, 10997.
- (3) Balch, A. L.; Holm, R. H. *J. Am. Chem. Soc.* **1966**, *88*, 5201.
- (4) Ghosh, P.; Begum, A.; Herebian, D.; Bothe, E.; Hildenbrand, K.; Weyhermüller, T.; Wieghardt, K. *Angew. Chem., Int. Ed.* **2003**, *42*, 563.
- (5) Bill, E.; Bothe, E.; Chaudhuri, P.; Chłopek, K.; Herebian, D.; Kokatam, S.; Ray, K.; Weyhermüller, T.; Neese, F.; Wieghardt, K. *Chem.—Eur. J.* **2005**, *11*, 204.
- (6) Warren, L. *Inorg. Chem.* **1977**, *16*, 2814.
- (7) Peng, S.-M.; Chen, C.-T.; Liaw, D.-S.; Chen, C.-I.; Wang, Y. *Inorg. Chim. Acta* **1985**, L31.
- (8) Christoph, G. G.; Goedken, V. L. *J. Am. Chem. Soc.* **1973**, *95*, 3869.
- (9) Chun, H.; Weyhermüller, T.; Bill, E.; Wieghardt, K. *Angew. Chem., Int. Ed.* **2001**, *40*, 2489.

To obtain a correct description of the molecular and electronic structure of such five-coordinate iron complexes with redox-noninnocent dioxolene type ligands we have investigated the coordination chemistry of *N*-phenyl-1,2-benzenediamine-derived ligands with iron ions in detail. The complexes synthesized here are listed in Scheme 1.

Experimental Section

The ligand *N*-phenylbenzene-1,2-diamine, $\text{H}_2[\text{L}^{\text{PDI}}]$, is commercially available (Aldrich) and was used as received. Unless otherwise stated all syntheses were performed under Ar atmosphere using a glovebox or standard Schlenk techniques.

$[\text{Fe}^{\text{III}}(\text{L}^{\text{ISQ}})(\text{L}^{\text{PDI}})]_2$ (**1**). To a solution of the ligand *N*-phenylbenzene-1,2-diamine, $[\text{L}^{\text{PDI}}]\text{H}_2$ (0.37 g; 2.0 mmol), in dry acetonitrile (7 mL) under an argon-blanketing atmosphere was added triethylamine (4.0 mmol) and $[\text{Fe}^{\text{III}}(\text{dmf})_6](\text{ClO}_4)_3$ ¹¹ (dmf = dimethylformamide) (0.79 g; 1.0 mmol). The resulting solution was stirred for 1 h at 20 °C. A black precipitate formed which was filtered off, washed with acetonitrile, and dried in vacuo. Yield: 0.19 g (45%). Mass spectrum (EI; m/z): 420; calcd for $\{\text{Fe}(\text{L}^{\text{ISQ}})_2\}^+$, 420.3. IR (KBr), cm^{-1} : $\nu(\text{N}-\text{H})$ 3316, 3296. Anal. Calcd for $\text{C}_{48}\text{H}_{40}\text{N}_8\text{Fe}_2$: C, 68.59; H, 4.80; N, 13.29; Fe, 13.33. Found: C, 68.5; H, 4.9; N, 13.2; Fe, 13.4.

$[\text{Fe}^{\text{II}}(\text{L}^{\text{ISQ}})_2(\text{PBu}_3)]$ (**2**). Complex **1** (0.18 g; 0.22 mmol) was suspended in acetonitrile (6 mL) under an Ar atmosphere. Tri-*n*-butylphosphane (0.10 g; 0.47 mmol) dissolved in 1 mL of CH_3CN was added dropwise. The resulting green solution was stirred at 20 °C for 30 min during which time a dark green precipitate formed. X-ray-quality single crystals were collected directly from the filtrate within 48 h. Yield: 0.17 g (63%). IR (KBr), cm^{-1} : $\nu(\text{N}-\text{H})$ 3307. Anal. Calcd for $\text{C}_{36}\text{H}_{47}\text{N}_4\text{FeP}$: C, 69.45; H, 7.61; N, 9.00; Fe, 8.97; P, 4.97. Found: C, 69.3; H, 7.6; N, 9.2; Fe, 9.0; P, 5.0.

$[\text{Fe}^{\text{III}}(\text{L}^{\text{ISQ}})_2(\text{PBu}_3)](\text{PF}_6)$ (**2^{ox}**). To a solution of **2** (154 mg; 0.247 mmol) in CH_2Cl_2 (6 mL) was added ferrocenium hexafluorophosphate (84 mg; 0.253 mmol) with stirring for 1.5 h at 20 °C. The dark green color of the solution immediately turned to dark blue. The resulting solution was filtered, and the filtrate was concentrated to ~1 mL by evaporation of the solvent under reduced pressure. *n*-Hexane (10 mL) was added, and the resulting suspension was stirred for 1 h. A dark blue precipitate formed, which was filtered off, washed with *n*-hexane (3×5 mL), and dried in vacuo. Single crystals suitable for X-ray crystallography were obtained by slow evaporation of $\text{CH}_2\text{Cl}_2/n$ -hexane solution (1:1 v/v) in a stream of argon. Yield: 0.10 g (54%). Mass spectrum (ESI, positive ion, CH_2Cl_2 ; m/z): 622, $\{2^{\text{ox}} - \text{PF}_6\}^+$. IR (KBr), cm^{-1} : $\nu(\text{N}-\text{H})$ 3307. Anal. Calcd for $\text{C}_{36}\text{H}_{47}\text{N}_4\text{F}_6\text{FeP}_2$: C, 56.33; H, 6.17; N, 7.30; F, 14.85; Fe, 7.28; P, 8.07. Found: C, 56.4; H, 6.1; N, 7.3; F, 15.0; Fe, 7.2; P, 8.1.

$[\text{Fe}^{\text{III}}(\text{L}^{\text{ISQ}})_2\text{I}]$ (**3**). To a stirred CH_2Cl_2 solution (5 mL) of **1** (175 mg; 0.21 mmol) under an argon-blanketing atmosphere was added iodine (53 mg; 0.21 mmol). The color of the solution immediately changed to dark violet. After the solution was stirred for 1 h, the solvent was removed by evaporation under reduced pressure to give a dark precipitate. Single crystals of **3**·THF were grown from a tetrahydrofuran solution of the crude material topped with diethyl ether (diffusion, 3:1 respectively, v/v). All spectroscopic investigations were carried out on powder samples of **3**. Yield: 167 mg (73%). MS (EI; m/z): 547 (M^+). IR (KBr), cm^{-1} : $\nu(\text{NH})$ 3317,

- (10) Chun, H.; Bill, E.; Weyhermüller, T.; Wieghardt, K. *Inorg. Chem.* **2003**, *42*, 5612.
- (11) Hodgkins, J.; Jordan, R. B. *J. Am. Chem. Soc.* **1973**, *95*, 763.

3277. Anal. Calcd for $C_{24}H_{20}N_4Fe$: C, 52.68; H, 3.68; N, 10.24; Fe, 10.21; I, 23.19. Found: C, 52.4; H, 3.9; N, 10.1; Fe, 10.2; I, 23.3.

[Fe^{II}(L^{ISQ})₂(CN-^tBu)] (4). To a solution of *tert*-butyl isocyanide (53 μ L; 0.46 mmol) in dry toluene (5 mL) was added a batch of **1** (175 mg; 0.21 mmol), whereupon the color of the solution changed rapidly to dark green. The mixture was stirred for 1 h at 20 °C. Within this time a brown precipitate formed, which was filtered off, washed with 3 mL of toluene, and dried in vacuo. Yield: 103 mg (49%). IR (KBr), cm^{-1} : $\nu(N-H)$ 3313; $\nu(CN)$ 2108. Anal. Calcd for $C_{29}H_{29}N_3Fe$: C, 69.19; H, 5.81; N, 13.91, Fe; 11.09. Found: C, 69.0; H, 5.7; N, 13.8; Fe, 11.4.

[Fe^{II}(L^{ISQ})₂(CNCy)] (5). To a solution of cyclohexyl isocyanide (48 mg; 0.44 mmol) in dry toluene (4 mL) was added a batch of **1** (179 mg; 0.21 mmol), whereupon the color of the solution changed rapidly to dark green. The mixture was stirred for 1 h at 20 °C. Within this time a brown precipitate formed, which was filtered off, washed with 3 mL of toluene, and dried in vacuo. Brown crystals suitable for X-ray crystallography were grown from toluene/dimethylacetamide (20:1 v/v) within 2 months at -18 °C. Yield: 115 mg (51%). IR (KBr), cm^{-1} : $\nu(N-H)$ 3313; $\nu(CN)$ 2213. Anal. Calcd for $C_{31}H_{30}N_3Fe(Fe_2O_3)_{0.5}$: C, 69.15; H, 5.99; N, 13.01; Fe, 10.37. Found: C, 69.2; H, 5.8; N, 12.9; Fe, 10.1.

[Fe^{III}(L^{ISQ})₂(Ph₂Im)] (6). 4,5-Diphenylimidazole,¹² H(Ph₂Im) (126 mg; 0.56 mmol), was suspended in dry toluene (4 mL), and **1** (114 mg; 0.27 mmol) was added with stirring in the presence of argon. Then acetonitrile (2 mL) was added. The resulting violet suspension was stirred at 20 °C for ~5 h. After filtration *n*-hexane was allowed to diffuse slowly into the liquid phase which afforded within 1 week black crystals of **6** of X-ray quality. Yield: 34 mg (20%). IR (KBr), cm^{-1} : $\nu(NH)$ 3316, 3301. Anal. Calcd for $C_{39}H_{31}N_6Fe$: C, 73.24; H, 4.89; N, 13.14; Fe, 8.73. Found: C, 73.2; H, 4.9; N, 13.0; Fe, 8.8.

[Fe^{III}(L^{ISQ})(L^{PD1})(BuPhCH-py)]·1.75BuPhCH-py (7·1.75BuPhCH-py). To a solution of 4-(1-phenylpentyl)pyridine¹³ (642 mg; 2.86 mmol) in dry toluene (5 mL) was added **1** (120 mg; 0.14 mmol). The resulting violet solution was allowed to stir at room temperature for 3 days. Then the solution was concentrated by evaporation of the solvent under reduced pressure. Dry *n*-hexane (10 mL) was added initiating precipitation of **2**. The suspension was stirred for an additional 30 min. Filtration of the resulting precipitate followed by washing with *n*-hexane (20 mL) gave a dark violet powder. The complex was recrystallized from toluene/*n*-hexane solution (diffusion, 1:1 v/v) within 1 week, affording needles of **7**·BuPhCH-py. All spectroscopic investigations were carried out on powder samples of **7**·1.75BuPhCH-py. Yield: 183 mg (62% with respect to **1**). IR (KBr), cm^{-1} : $\nu(NH)$ 3318. Anal. Calcd for $C_{40}H_{39}N_5Fe\cdot 1.75C_{16}H_{19}N$: C, 78.54; H, 7.00; N, 9.09; Fe, 5.37. Found: C, 78.5; H, 7.0; N, 9.1; Fe, 5.4.

[C₂₄H₁₉N₄](ClO₄) (8). To a solution of *N*-phenyl-1,2-benzenediamine (368 mg; 2 mmol) in acetonitrile (10 mL) was added triethylamine (4 mmol) under argon followed by addition of [Fe^{III}(dmf)₆](ClO₄)₃ (0.79 g; 1 mmol). The solution was stirred for 10 min at room temperature and then exposed to air for 30 s. A dark-violet-brown solution was obtained and was left for 2 days in the closed flask at 20 °C. Dark red-brown crystals suitable for X-ray crystallography formed that were collected and washed with acetonitrile. Yield: 278 mg (60%). Mass spectrum (ESI, positive ion, CH₂Cl₂; *m/z*): 363, {8 - ClO₄}⁺.

(12) McMaster, J.; Beddoes, R. L.; Collison, D.; Eardley, D. R.; Helliwell, M.; Garner, C. D. *Chem.—Eur. J.* **1996**, *2*, 685.

(13) Sperber, N.; Papa, D.; Bloomfield, N. J. (Schering Corp.) U.S. Patent 2727895, 1955.

X-ray Crystallographic Data Collection and Refinement of the Structures. Dark brown single crystals of **2** and **6**, black crystals of **2^{ox}**, **3** and **7**, and dark red crystals of **5** and **8** were coated with perfluoropolyether and mounted in the nitrogen cold stream of a Nonius Kappa-CCD diffractometer equipped with a Mo-target rotating-anode X-ray source and a graphite monochromator (Mo K α , $\lambda = 0.71073$ Å). Final cell constants were obtained from least-squares fits of all measured reflections. Crystal faces were determined, and the corresponding intensity data were corrected for absorption using the Gaussian-type routine embedded in XPREP.¹⁴ The Siemens ShelXTL¹⁴ software package was used for solution and artwork of the structure, and ShelXL97¹⁵ was used for the refinement. The structures were readily solved by direct and Patterson methods and subsequent difference Fourier techniques. All non-hydrogen atoms were refined anisotropically. Hydrogen atoms attached to carbon atoms were placed at calculated positions and refined as riding atoms with isotropic displacement parameters. Crystallographic data of the compounds are listed in Table 1. The apical ligand of compound **7** was found to be disordered. Two split positions representing the two enantiomers were refined in a 2:1 ratio. Chemically equal atoms were restrained to have the same anisotropic displacement parameters (EADP) and similar bond distances (SADI).

Physical Measurements. The equipment used for IR, UV-vis, EPR, and Mössbauer spectroscopies has been described in refs 16 and 17. The temperature-dependent magnetic susceptibilities of solid samples of complexes were measured by using a SQUID magnetometer (Quantum Design) at 1.0 T magnetic field in the range 2.0–300 K. Corrections for underlying diamagnetism were made by using tabulated Pascal's constants. Spin Hamiltonian simulations of EPR spectra were performed with the XSOPHE program written by Hanson et al., which is distributed by Bruker Biospin GmbH. Ligand hyperfine interactions, including quadrupole interactions, were considered with the full-matrix approach. Cyclic voltammetry and coulometric experiments were performed using an EG&G potentiostat/galvanostat.

Results

1. Synthesis of Complexes. The reaction of the ligand *N*-phenyl-1,2-benzenediamine, H₂[L^{PD1}], with [Fe^{III}(dmf)₆](ClO₄)₃ (dmf = dimethylformamide) in the ratio 2:1 in acetonitrile solution in the presence of 4 equiv of triethylamine under strictly anaerobic conditions at ambient temperature yields a black, diamagnetic precipitate of the dimer [Fe^{III}(L^{ISQ})(L^{PD1})₂ (**1**) in 45% yield. Remarkably, other ferric salts such as Fe(acac)₃, FeCl₃, or Fe(ClO₄)₃·9H₂O or ferrous salts do not react with H₂[L^{PD1}] in acetonitrile under the same conditions as described above. The dark violet product **1** is quite sensitive toward oxygen both in solution and in the solid state. The reaction of [Fe^{III}(dmf)₆](ClO₄)₃ with H₂[L^{PD1}] in acetonitrile in the presence of air and NEt₃ affords rapidly the deep red, benzoquinone **8**.

The formation of **1** is accompanied by a one-electron oxidation of (L^{PD1})²⁻ yielding the monoanionic π radical (L^{ISQ})^{•-} and concomitant reduction of a ferric ion as shown schematically in eq 1, which is in agreement with the

(14) ShelXTL, V.5; Siemens Analytical X-ray Instruments, Inc.: Madison, WI, 1994.

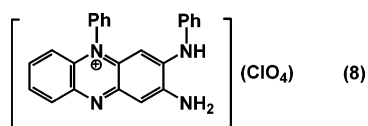
(15) Sheldrick, G. M. *ShelXL97*; University of Göttingen: Göttingen, Germany, 1997.

Table 1. Crystallographic Data for **2**, **2^{ox}**, **3**·THF, **5**, **6**, **7**·C₁₆H₁₉N, and **8**

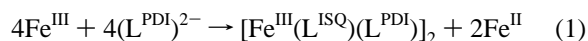
param	2	2^{ox}	3 ·THF	5
chem formula	C ₃₆ H ₄₇ FeN ₄ P	C ₃₆ H ₄₇ F ₆ FeN ₄ P ₂	C ₂₈ H ₂₈ FeIN ₄ O	C ₃₁ H ₃₁ FeN ₅
fw	622.60	767.57	619.29	529.46
space group, No.	P1, 2	P2 ₁ /c, 14	P2 ₁ 2 ₁ 2 ₁ , 19	P1, 2
a, Å	8.7205(6)	11.5157(3)	8.8303(3)	9.7055(3)
b, Å	18.7990(10)	19.7687(3)	8.9151(3)	10.1735(3)
c, Å	20.008(2)	16.9228(3)	32.2025(8)	13.8527(6)
α, deg	99.49(1)	90	90	85.01(1)
β, deg	90.83(1)	106.98(1)	90	71.42(1)
γ, deg	91.99(1)	90	90	75.98(1)
V, Å ³	3232.5(4)	3684.54(13)	2535.08(14)	1257.82(8)
Z	4	4	4	2
T, K	100(2)	100(2)	100(2)	100(2)
ρ _{calcd} , g cm ⁻³	1.279	1.384	1.623	1.398
reflens collcd/2θ _{max} , deg	43472/45.00	103 666/66.00	47 100/67.44	31 963/62.00
unique reflens/I > 2σ(I)	8427/6006	13 872/11 345	9941/9245	7970/7207
no. of params/restr	757/0	450/0	322/1	334/1
λ, Å /μ(Kα), cm ⁻¹	0.710 73/5.47	0.710 73/5.58	0.710 73/18.41	0.710 73/6.30
R1 ^a /goodness of fit ^b	0.0534/1.074	0.0350/1.024	0.0286/1.042	0.0579/1.047
wR2 ^c (I > 2σ(I))	0.0924	0.0770	0.0599	0.1390
resid density, e Å ⁻³	+0.47/-0.33	+0.48/-0.35	+0.77/-0.67	+4.31/-1.48

param	6	7 ·C ₁₆ H ₁₉ N	8
chem formula	C ₃₉ H ₃₁ FeN ₆	C ₅₆ H ₅₈ FeN ₆	C ₂₄ H ₁₉ ClN ₄ O ₄
fw	639.55	870.93	462.88
space group, No.	P2 ₁ /n, 14	P1, 2	P1, 2
a, Å	10.4433(3)	10.0549(4)	8.1962(6)
b, Å	17.7647(6)	13.2152(8)	10.7105(9)
c, Å	17.0145(6)	18.2622(10)	13.3665(12)
α, deg	90	90.92(1)	68.48(1)
β, deg	98.334(5)	104.33(1)	73.00(1)
γ, deg	90	100.85(1)	85.10(1)
V, Å ³	3123.2(2)	2304.1(2)	1043.6(2)
Z	4	2	2
T, K	100(2)	100(2)	100(2)
ρ _{calcd} , g cm ⁻³	1.360	1.255	1.473
reflens collcd/2θ _{max} deg	75693/61.96	27561/50.0	7128/50.00
unique reflens/I > 2σ(I)	9890/8309	8064/5813	3632/2908
no. of params/restr	421/1	566/18	307/0
λ, Å /μ(Kα), cm ⁻¹	0.710 73/5.22	0.710 73/3.72	0.710 73/2.25
R1 ^a /goodness of fit ^b	0.0434/1.075	0.0668/1.029	0.0397/1.040
wR2 ^c (I > 2σ(I))	0.0934	0.1312	0.0860
resid density, e Å ⁻³	+0.44/-0.39	+0.75 /-0.76	+0.24/-0.41

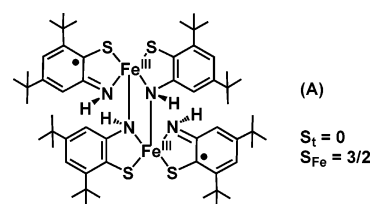
^a Observation criterion: $I > 2\sigma(I)$. $R1 = \sum||F_o| - |F_c||/\sum|F_o|$. ^b GooF = $[\sum[w(F_o^2 - F_c^2)^2]/(n - p)]^{1/2}$. ^c wR2 = $[\sum[w(F_o^2 - F_c^2)^2]/\sum[w(F_o^2)^2]]^{1/2}$, where $w = 1/\sigma^2(F_o^2) + (aP)^2 + bP$ and $P = (F_o^2 + 2F_c^2)/3$.



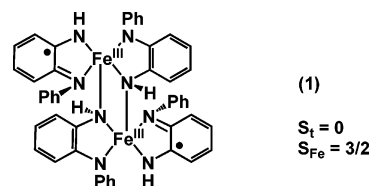
observation that the yields of **1** never exceed 50% of the starting material $[\text{Fe}^{\text{III}}(\text{dmf})_6](\text{ClO}_4)_3$.



The electronic spectra and the Mössbauer parameters of **1** (see below) are very similar to those reported for the structurally characterized complex **A**.¹⁶ From magnetic susceptibility measurements (3–300 K) it is established that both **1** and **A** are diamagnetic. Therefore, we propose that **1** consists of two square planar $[\text{Fe}^{\text{III}}(\text{L}^{\text{PDI}})(\text{L}^{\text{ISQ}})]$ halves which are bridged by two R–NH groups one of each N, N' -coordinated $(\text{L}^{\text{PDI}})^{2-}$. The two nonbridging ligands are the $(\text{L}^{\text{ISQ}})^{\cdot-}$ π radicals. The spin of this ligand radical ($S_{\text{rad}} = 1/2$) couples



antiferromagnetically to an intermediate-spin ferric ion ($S_{\text{Fe}} = 3/2$), and the two halves $[\text{Fe}^{\text{III}}(\text{L}^{\text{PDI}})(\text{L}^{\text{ISQ}})]$ each with an $S^* = 1$ state couple strongly antiferromagnetically in the dimer yielding the observed diamagnetic ground state.

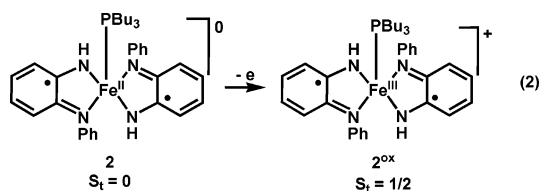


Complex **1** has proven to be a useful starting material for the synthesis of the following five-coordinate mononuclear complexes. Thus, the reaction of the dimer **1** with tri- n -

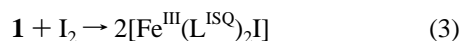
(16) Ghosh, P.; Bill, E.; Weyhermüller, T.; Wieghardt, K. *J. Am. Chem. Soc.* **2003**, *125*, 3967.

butylphosphane, $\text{P}(\text{Bu})_3$ (ratio 1:2), in acetonitrile affords a dark green precipitate of mononuclear $[\text{Fe}^{\text{II}}(\text{L}^{\text{ISQ}})_2(\text{PBu}_3)]$ (**2**) under anaerobic conditions. Formally, this represents a simple addition reaction. Complex **2** is diamagnetic with an $S_{\text{t}} = 0$ ground state as was shown from applied field Mössbauer spectroscopy and magnetic susceptibility measurements (3–300 K). Upon addition of the phosphane the electronic structure of the FeL_2 -structural unit changes from $[\text{Fe}^{\text{III}}(\text{L}^{\text{PDI}})(\text{L}^{\text{ISQ}})]$ in **1** to $[\text{Fe}^{\text{II}}(\text{L}^{\text{ISQ}})_2]$ in **2** via intramolecular one-electron transfer with reduction of the ferric ion and oxidation of the $(\text{L}^{\text{PDI}})^{2-}$. Strong antiferromagnetic interligand spin exchange coupling via a low-spin ferrous ion ($S_{\text{Fe}} = 0$) could yield the diamagnetic ground state in mononuclear **2**, but see also the alternative models discussed below.

It is interesting that **2** can be one-electron oxidized by using 1 equiv of ferrocenium hexafluorophosphate in CH_2Cl_2 under anaerobic conditions yielding dark blue crystals of $[\text{Fe}^{\text{III}}(\text{L}^{\text{ISQ}})_2(\text{PBu}_3)](\text{PF}_6)$ (**2^{ox}**, eq 2). Note that this complex **2^{ox}** represents the exact analogue of Warren's complex $[\text{Fe}\{o\text{-C}_6\text{H}_4(\text{NH})_2\}_2(\text{PPh}_3)](\text{PF}_6)$ ($S_{\text{t}} = 1/2$).⁶ Figure S1 (top) (Supporting Information) displays the temperature dependence of the magnetic moment of **2^{ox}** which reveals an $S = 1/2$ ground state. The solid line represents a best fit using the following parameters: $g_{\text{iso}} = 2.12$; a temperature-independent paramagnetism (χ_{TIP}) of 241×10^{-6} emu; a paramagnetic impurity ($S = 5/2$) of 0.9%; Weiss constant Θ of -1.50 K indicating weak intermolecular antiferromagnetic exchange coupling.



Similarly, oxidation of **1** with iodine (1:1) under anaerobic conditions in CH_2Cl_2 solution affords the neutral, black complex $[[\text{Fe}^{\text{III}}(\text{L}^{\text{ISQ}})_2]\text{I}]$ (**3**) in good yields, eq 3.



Complex **3** is again the exact analogue of Warren's complex⁶ $[\text{Fe}^{\text{III}}\{o\text{-C}_6\text{H}_4(\text{NH})_2\}_2\text{I}]$ ($S_{\text{t}} = 1/2$). The temperature dependence of the magnetic moment of **3** shown in Figure S1 (middle) indicates a doublet ground state ($S_{\text{t}} = 1/2$). The best fit was obtained by using the following parameters: a Weiss constant Θ of -2.6 K indicating weak intermolecular spin exchange coupling; $g_{\text{iso}} = 2.11$; $\chi_{\text{TIP}} = 67 \times 10^{-6}$ emu.

Addition of 2 equiv of an isocyanide (*tert*-butyl or cyclohexyl isocyanide) to a toluene solution of **1** (ratio 2:1) under anaerobic conditions produces brown precipitates of $[\text{Fe}^{\text{II}}(\text{L}^{\text{ISQ}})_2(\text{CN}^-\text{tBu})]$ (**4**) and $[\text{Fe}^{\text{II}}(\text{L}^{\text{ISQ}})_2(\text{CNCy})]$ (**5**), respectively, both of which possess an $S_{\text{t}} = 0$ ground state. The electronic structure of **4** and **5** is the same as that of **2**.

The same reaction using the ligand 4,5-diphenylimidazole yields the neutral complex $[\text{Fe}^{\text{III}}(\text{L}^{\text{ISQ}})_2(\text{Ph}_2\text{Im})]$ (**6**), where $(\text{Ph}_2\text{Im})^-$ represents the deprotonated monoanionic form of the ligand 4,5-diphenylimidazole. The temperature depen-

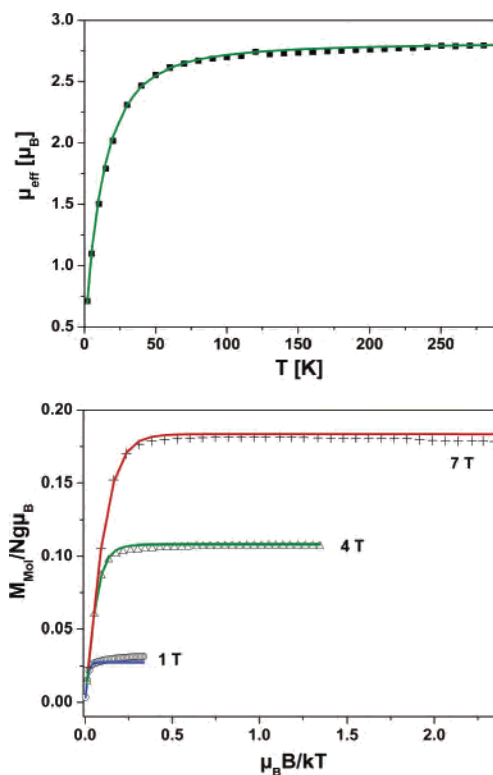
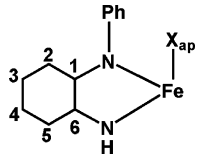


Figure 1. Temperature dependence of the magnetic moment, μ_{eff} , of a solid sample of **7** recorded in a 1.0 T magnetic field (top) and variable-field and variable-temperature dependence of the magnetization of **7** (bottom). The solid lines represent best fits using the parameters given in the text.

dence of the magnetic moment of **6** shown in Figure S1 (bottom) indicates again an $S_{\text{t}} = 1/2$ ground state. The best fit was obtained by using the following parameters: $g_{\text{iso}} = 2.1$ (fixed); $\chi_{\text{TIP}} = 386 \times 10^{-6}$ emu; a Weiss constant Θ of -16.0 K or, alternatively, a coupling constant $J = -11.4$ cm^{-1} ($H = -2JS_1 \cdot S_2$; $S_1 = S_2 = 1/2$) for a dimer model.

Finally, we have studied the reaction of racemic 4-(1-phenylpentyl)pyridine (BuPhCH-py) with **1** in dry toluene (ratio 2:1). From the resulting violet solution to which *n*-hexane had been added a dark violet precipitate of $[\text{Fe}^{\text{III}}(\text{L}^{\text{ISQ}})(\text{L}^{\text{PDI}})(\text{BuPhCH-py})] \cdot 1.75\text{BuPhCH-py}$ (**7**) was obtained. The electronic structure of this addition product **7** differs from that of diamagnetic **2**, **4**, and **5**. From variable-temperature (2–295 K) magnetic susceptibility measurements and from variable-field (1, 4, 7 T) and variable-temperature magnetization measurements shown in Figure 1 a triplet ground state ($S_{\text{t}} = 1$) for **7** has been established. The fits in Figure 1 were obtained by using the following parameters: $g = 2.0$ (fixed); $D = +48$ cm^{-1} ; $E/D = 0.22$. Assuming the presence of an intermediate spin ferric ion ($S_{\text{Fe}} = 3/2$) and a single strongly antiferromagnetically coupled $(\text{L}^{\text{ISQ}})^-\pi$ radical, the $S_{\text{t}} = 1$ ground state is obtained. From spin projection techniques one can evaluate the corresponding intrinsic parameter for the iron ion D_{Fe} from the relation $D_{\text{Fe}} (S_{\text{Fe}} = 3/2) = 2/3 D (S_{\text{t}} = 1) = 32$ cm^{-1} . The solid lines in Figure 1 represent spin Hamiltonian simulations for an $S_{\text{t}} = 1$ system, eq 4.

$$H = D[S_z^2 - S(S+1)/3 + E/D(S_x^2 - S_y^2)] + \mu_{\text{B}} B g S \quad (4)$$

Table 2. Selected Bond Lengths (Å) of Complexes (averaged)


bond	2	2 ^{ox}	3	5	6	7
Fe–N _{Ph}	1.923(3)	1.903(1)	1.904(2)	1.909(2)	1.906(1)	1.893(3)
Fe–N _H	1.868(3)	1.865(1)	1.877(2)	1.876(2)	1.876(1)	1.873(3)
Fe–X _{ap}	2.221(1)	2.3326(3)	2.5984(3)	1.840(2)	1.974(1)	2.190(3)
C1–C2	1.406(6)	1.418(2)	1.418(3)	1.415(2)	1.422(2)	1.405(5)
C2–C3	1.374(6)	1.375(2)	1.376(3)	1.379(3)	1.374(2)	1.377(5)
C3–C4	1.404(6)	1.419(2)	1.418(3)	1.416(3)	1.422(3)	1.400(5)
C4–C5	1.372(6)	1.373(2)	1.370(3)	1.376(3)	1.372(2)	1.377(5)
C5–C6	1.415(6)	1.419(2)	1.422(3)	1.416(2)	1.419(2)	1.402(5)
C6–C1	1.425(6)	1.433(2)	1.436(3)	1.434(2)	1.434(2)	1.426(5)
C1–N _{Ph}	1.371(5)	1.360(1)	1.356(3)	1.356(2)	1.358(2)	1.371(5)
C6–N _H	1.356(5)	1.342(1)	1.341(2)	1.346(2)	1.342(2)	1.353(4)

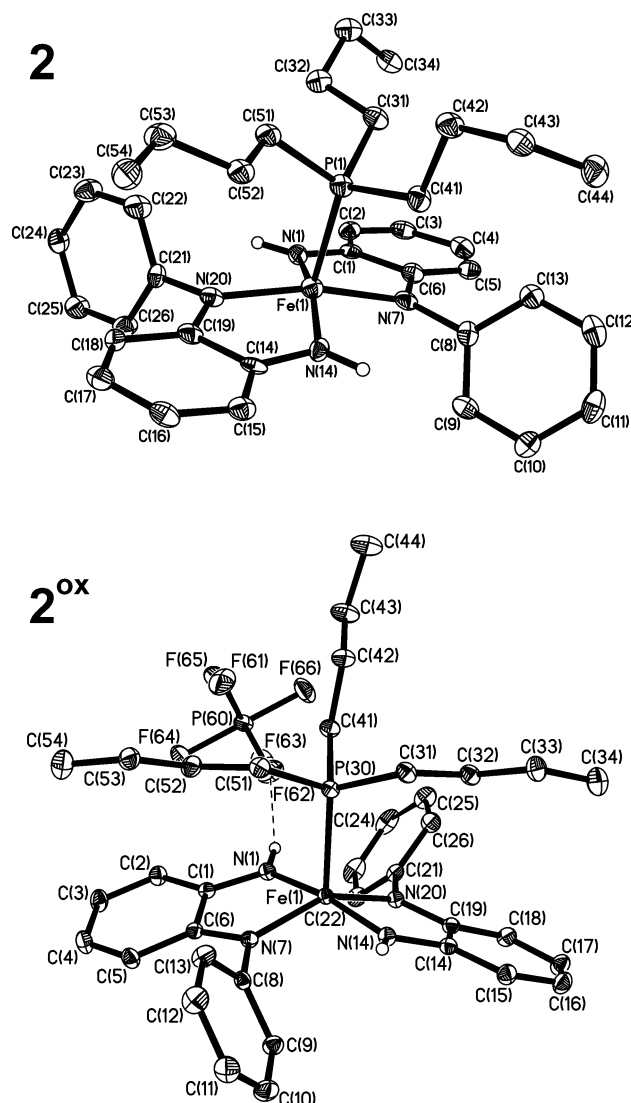
Note that diamagnetic **4** and **5** contain the redox isomeric chromophore $[\text{Fe}^{\text{II}}(\text{L}^{\text{ISQ}})_2\text{X}]$ with a low-spin ferrous ion and two antiferromagnetically coupled ligand radicals. Complex **7**, on the other hand, has the same chromophore as complex **1**, and consequently, their electronic spectra are very similar (see below).

2. Crystal Structures. The crystal structures of **2**, **2^{ox}**, **3**, and **5–7** have been determined by single-crystal X-ray crystallography at 100 K. Table 1 gives crystallographic data, and Table 2 summarizes important bond lengths.

Figure 2 displays the neutral molecule in crystals of **2** (top) and the ion pair $[\text{Fe}(\text{L}^{\text{ISQ}})_2(\text{PBU}_3)](\text{PF}_6)$ in crystals of **2^{ox}** (bottom). The neutral species and the corresponding monocation consist both of an iron ion in a square pyramidal coordination sphere composed of two *N,N*-coordinated $\{\text{C}_6\text{H}_4(\text{NH},\text{NPh})\}^{\pi-}$ ligands in equatorial positions and a single PBU_3 ligand in the apical position. It is now quite remarkable that the C–C and C–N distances of both ligands in both **2** and **2^{ox}** are within experimental error identical; the respective bond lengths are identical with those reported for the square planar singlet diradical complexes $[\text{M}^{\text{II}}(\text{L}^{\text{ISQ}})_2]$ ($\text{M} = \text{Ni},^{2a} \text{Pd},^{2a} \text{Co}^5$) all of which contain two *N*-phenyl-*o*-diiminobenzosemiquinonate(1[−]) π radicals. We interpret this as strong evidence that in both **2** and **2^{ox}** also two radical monoanions are present which, in turn, indicates that the iron ion in **2** is a ferrous ion but in **2^{ox}** it is a ferric ion. Thus, the one-electron oxidation of **2** to **2^{ox}** is a metal-centered process.

The above notion is corroborated by the following observations: The four Fe–N bond distances in **2** and **2^{ox}** are nearly identical (average Fe–N_{Ph} 1.91 Å and Fe–N_H 1.87 Å). The ionic radii of the ferrous ion in **2** and of the ferric ion in **2^{ox}** must be very similar. This is expected to be true for a low- or intermediate-spin ferrous ion ($S_{\text{Fe}} = 0$ or 1) and an intermediate-spin ferric ion ($S_{\text{Fe}} = 3/2$). The phosphane ligand in the apical position is a π acceptor, and the Fe–P bond lengths in **2** and **2^{ox}** are expected to differ. This is indeed the case. In **2** the Fe–P bond distance at 2.221 ± 0.003 Å is significantly shorter than the same bond in **2^{ox}** at 2.332 ± 0.001 Å due to the fact that a ferrous ion is a better π back-bonding system than the corresponding system of an intermediate spin ferric ion.

The neutral mononuclear complex in crystals of **3**·THF is shown in Figure 3 (top). Clearly, the geometrical features of the two identical ligands (L^{ISQ}^-) are consistent only with a formulation as π radical monoanions ($\text{L}^{\text{ISQ}}\bullet^-$) which renders

**Figure 2.** Crystal structures of the neutral complex in crystals of **2** (top) and of an ion pair in crystals of **2^{ox}** (bottom).

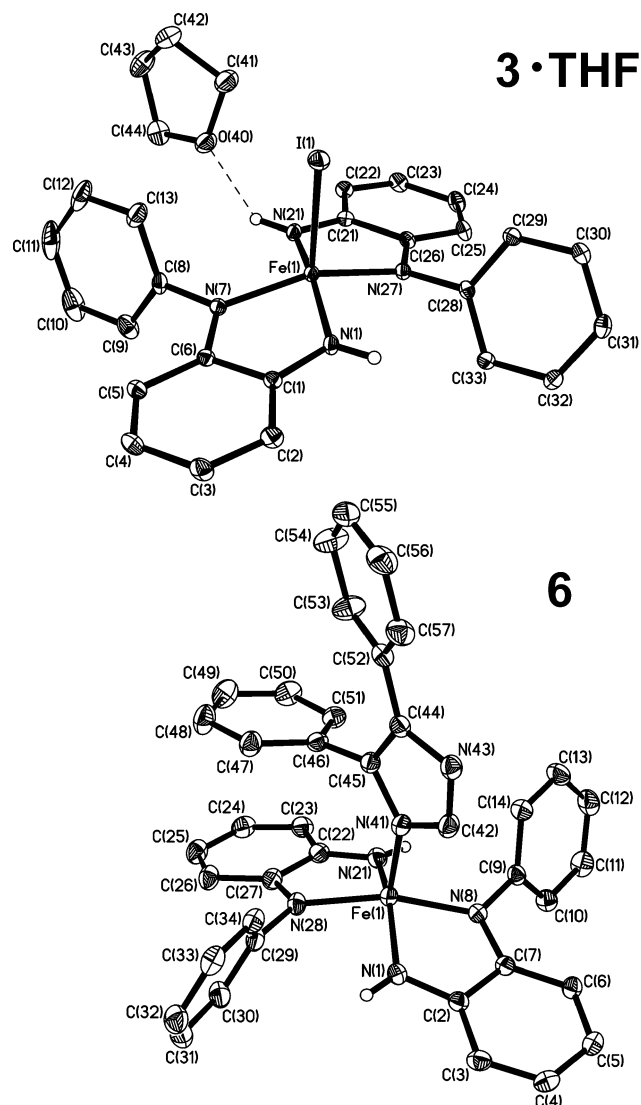


Figure 3. Crystal structures of neutral $[\text{Fe}^{\text{III}}(\text{L}^{\text{ISQ}})_2]$ in crystals of **3**·THF (top) and of $[\text{Fe}^{\text{III}}(\text{L}^{\text{ISQ}})_2(\text{Ph}_2\text{Im})]$ in crystals of **6** (bottom).

the central iron ion trivalent ($S_{\text{Fe}} = 3/2$). The Fe–N distances of the FeN_4 core are identical with those in **2** and 2^{ox} . Complex **3** is therefore to be described as $[\text{Fe}^{\text{III}}(\text{L}^{\text{ISQ}})_2]$ where the central ferric ion with an intrinsic $S_{\text{Fe}} = 3/2$ ground state couples strongly in an antiferromagnetic fashion to the spins of the two ligand radicals ($S_{\text{rad}} = 1/2$) yielding the observed $S_{\text{t}} = 1/2$ ground state. The structure of diamagnetic $[\text{Co}^{\text{III}}(\text{L}^{\text{ISQ}})_2]\cdot\text{THF}$ is similar.⁵

The structure of the neutral, diamagnetic isocyanide complex $[\text{Fe}^{\text{II}}(\text{L}^{\text{ISQ}})_2(\text{CNCy})]$ (**5**) is shown in Figure 4 (top). It is satisfying that the geometrical features of the $\text{Fe}^{\text{II}}(\text{L}^{\text{ISQ}})_2$ chromophore are identical with those found in isoelectronic **2** (Table 2).

The neutral complex $[\text{Fe}^{\text{III}}(\text{L}^{\text{ISQ}})_2(\text{Ph}_2\text{Im})]$ (**6**) is shown in Figure 3 (bottom). Again, the geometrical details of the $\text{Fe}^{\text{III}}(\text{L}^{\text{ISQ}})_2$ chromophore indicate the presence of two N,N' -coordinated N -phenyl-*o*-diiminobenzosemiquinonate(1[−]) π radicals. A deprotonated 4,5-diphenylimidazole(1[−]) monoanion occupies the apical position in the square base pyramidal coordination polyhedron. Simple charge considerations imply then the presence of a central ferric ion. The observed $S_{\text{t}} =$

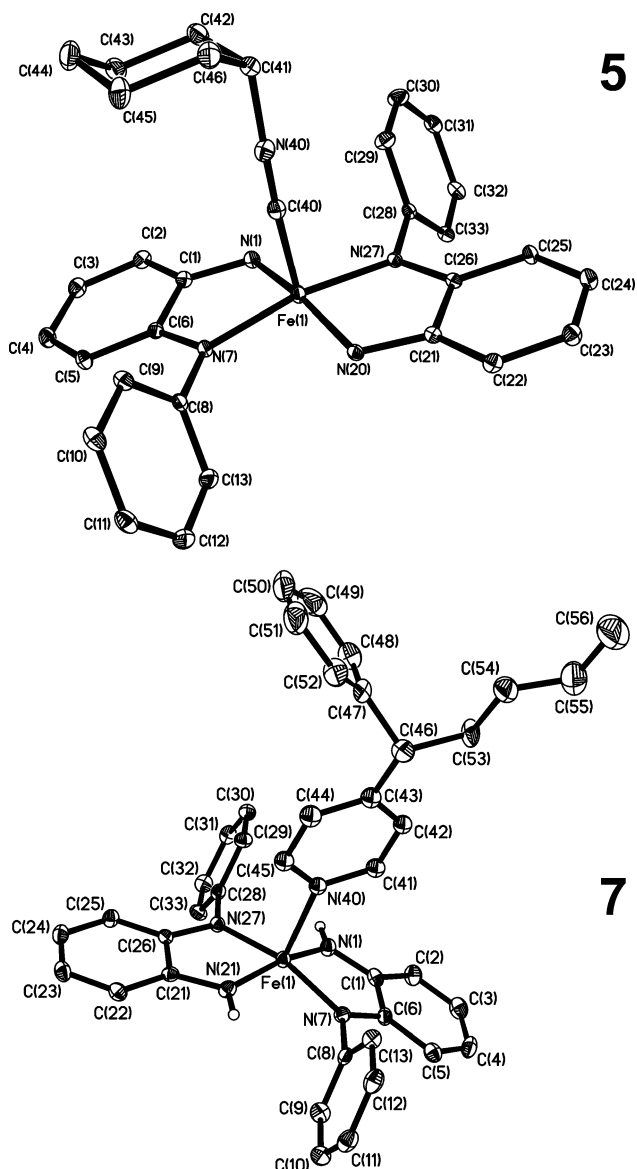


Figure 4. Crystal structures of neutral $[\text{Fe}^{\text{II}}(\text{L}^{\text{ISQ}})_2(\text{CNCy})]$ in crystals of **5** (top) and of $[\text{Fe}^{\text{II}}(\text{L}^{\text{ISQ}})(\text{L}^{\text{PDI}})(\text{BuPhCH-py})]$ in crystals of **7** (bottom).

$1/2$ ground state of **6** is achieved via strong antiferromagnetic coupling of an intermediate-spin ferric ion with two ligand radicals as in 2^{ox} and **3**.

The structure of $[\text{Fe}^{\text{II}}(\text{L}^{\text{ISQ}})(\text{L}^{\text{PDI}})(\text{BuPhCH-py})]$ in crystals of **7**·BuPhCH-py is shown in Figure 4 (bottom). The dimensions of the $\text{Fe}^{\text{II}}(\text{L}^{\text{ISQ}})(\text{L}^{\text{PDI}})$ chromophore are slightly different from those of all $\text{Fe}^{\text{II/III}}(\text{L}^{\text{ISQ}})_2$ chromophores in **2**, 2^{ox} , **3**, **5**, and **6**. The data for the C–C and C–N bond lengths are in agreement with the arithmetic mean values between an $(\text{L}^{\text{ISQ}})^{\cdot-}$ and an $(\text{L}^{\text{PDI}})^{2-}$ ligand, but it is not quite possible using exclusively X-ray structural data to discern between an $\text{Fe}^{\text{II/III}}(\text{L}^{\text{ISQ}})_2$ and an $\text{Fe}^{\text{III}}(\text{L}^{\text{ISQ}})(\text{L}^{\text{PDI}})$ chromophore with the ligand mixed valency being of the delocalized class III type.

The square pyramidal (sp) coordination of complexes exhibits in a few cases a slight distortion toward a trigonal bipyramidal (tbp) coordination sphere. The degree of this distortion may be expressed by the τ parameter as defined by Addison et al. (*J. Chem. Soc., Dalton Trans.* **1984**, 1349)

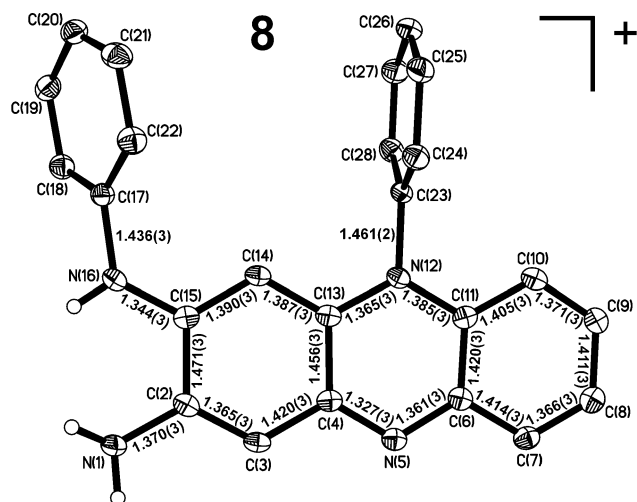


Figure 5. Crystal structure of the monocation in crystals of **8** and bond distances in Å.

Table 3. Cyclic Voltammograms of Complexes in CH₂Cl₂ (0.10 M [N(*n*-Bu)₄]PF₆) at 20 °C (Glassy Carbon Working Electrode; Scan Rate 200 mV s⁻¹)^a

complex	<i>T</i> , K	<i>E</i> _{p,ox} , V	<i>E</i> _{1/2} , V	<i>E</i> _{p,red} , V	<i>E</i> _{p,red} , V
2	298	0.46 (irr)	-0.75 (r)	-1.66 (irr)	nm
4	253	0.45 (irr)	-0.58 (r)	-1.54 (irr)	-2.02 (irr)
5	253	0.47 (irr)	-0.57 (r)	-1.52 (irr)	-2.02 (irr)

^a Redox potentials are referenced in V vs the ferrocenium/ferrocene couple.

which is zero for *sp* and unity for *tbp*. For **2** τ is 0.00, for **2^{ox}** 0.37, for **3** 0.06, for **5** 0.00, for **6** 0.16, and for **7** 0.03.

Finally, Figure 5 shows the structure of the monocation in crystals of **8**.

3. Electro- and Spectroelectrochemistry. The electrochemical activity of complexes **2**, **4**, and **5** has been studied by cyclic voltammetry in CH₂Cl₂ solutions containing 0.10 M [N(*n*-Bu)₄]PF₆ as supporting electrolyte. All redox potentials are referenced vs the ferrocenium/ferrocene, Fc⁺/Fc, couple; the results are summarized in Table 3. All three isoelectronic species exhibit a reversible one-electron-transfer wave at -0.57 V for **5**, -0.58 V for **4**, and -0.75 V for **2**, for the couple [complex]⁺/[complex]⁰. In addition, each species displays an irreversible oxidation at ~+0.5 V and an irreversible reduction at -1.6 V. These processes were not further investigated. Controlled potential coulometry at -0.3 V of CH₂Cl₂ solutions of **2**, **4**, and **5** established that these species are oxidized by 1.0 ± 0.1 electrons generating the stable monocations **2^{ox}**, **4^{ox}**, and **5^{ox}**, respectively. The electronic spectra at 249 K of the electrochemically generated species as well as of their starting complexes have been recorded. Table 4 summarizes the results.

It is of great interest that the spectra of all of these complexes are dominated by the oxidation level of the respective Fe(L)₂ chromophore; they appear to be nearly independent of the nature of the apical ligand.

As shown in Figure 6 (top) the electronic spectra of **1** and **7** are very similar. We suggest that they are indicative of the [Fe^{III}(L^{ISQ})(L^{PDl})] chromophore. Similarly, the spectra of **2**, **4**, and **5** displayed in Figure 6 (middle) are very similar

Table 4. Electronic Spectra of Complexes in CH₂Cl₂ Solution

complex	<i>T</i> , K	λ_{\max} , nm (ϵ , 10 ⁴ M ⁻¹ cm ⁻¹)
1	298	410 sh (0.6), 500 (1.02), 647 (0.68), 774 sh (0.4)
2	249	290 sh (2.2), 472 (1.1), 587 (0.6), 718 (2.2)
2^{ox}	249	406 (0.9), 491 (1.7), 603 (1.6), 685 sh (0.6), 820 sh (0.2)
3	298	471 sh (1.6), 524 (2.6), 568 sh (1.8), 610 (1.9)
4	249	419 sh (0.7), 462 (0.9), 497 sh (0.8), 567 (0.6), 703 (2.0)
4^{ox}	249	409 (0.5), 504 (1.0), 631 (0.8)
5	249	302 (1.2), 422 sh (0.6), 456 (0.8), 513 (0.4), 570 (0.4), 706 (2.1)
5^{ox}	249	418 (0.4), 511 (1.0), 607 (0.6), 698 sh (0.3)
6	298	270 (2.4), 407 (0.8), 499 (1.9), 640 (0.6)
7	298	494 (0.9), 658 (0.6), 889 sh (0.3)

^a Electrochemically generated at 249 K in CH₂Cl₂ (0.10 M [N(*n*-Bu)₄]PF₆).

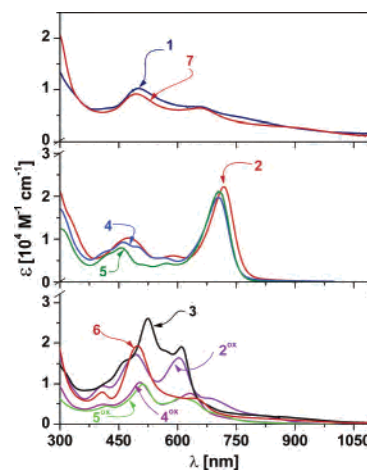


Figure 6. Electronic spectra of complexes in CH₂Cl₂ solution at ambient temperature: (top) spectra of **1** and **7**; (middle) spectra of **2**, **4**, and **5**; (bottom) spectra of **2^{ox}**, **3**, **4^{ox}**, **5^{ox}**, and **6**.

with an intense ligand-to-ligand charge-transfer band (LLCT) at ~710 nm which is characteristic for the [Fe^{II}(L^{ISQ})₂] chromophore. Finally, the spectra of **2^{ox}**, **3**, **4^{ox}**, **5^{ox}**, and **6** are very similar; they all exhibit two intense CT bands at ~500 and ~620 nm. These spectra are characteristic of the Fe^{III}(L^{ISQ})₂ chromophore.

In Table 5 a summary of all structurally characterized five-coordinate iron complexes containing π radical monoanions and their one-electron-reduced, closed-shell dianions of *o*-phenylenediamine, (L_{NN})ⁿ, *o*-aminothiophenol, (L_{N,S})ⁿ,¹⁶ benzene-1,2-dithiol, (L_{S,S})ⁿ,¹⁷ and *o*-aminophenol, (L_{N,O})ⁿ,^{9,10} is given. It is quite remarkable that irrespective of the nature of the ligands the electronic spectra are characteristic for a given chromophore: type I, [Fe^{II}(L[•])₂]; type II, [Fe^{III}(L[•])(L)]; type III, [Fe^{III}(L[•])₂]. This indicates that all species belonging to a given type have the same electronic structure.

4. EPR Spectroscopy. All mononuclear complexes containing an [Fe^{III}(L^{ISQ})₂] chromophore as in **2^{ox}**, **3**, **4^{ox}**, **5^{ox}**, and **6** possess an *S*_t = 1/2 ground state as has been established by their X-band EPR spectra recorded at 8–30 K in frozen acetonitrile/toluene (1:1) mixtures (**2^{ox}**, **3**) or CH₂Cl₂ solution (**4^{ox}**, **5^{ox}**) or in a CH₂Cl₂/toluene mixture (**6**). The results are given in Table 6, and Figure 7 (top) shows a typical example. In a previous analysis of similar compounds we analyzed such rhombic EPR spectra with all *g* values *g* > 2 in

(17) Ray, K.; Bill, E.; Weyhermüller, T.; Wieghardt, K. *J. Am. Chem. Soc.* **2005**, *127*, 5641.

Table 5. Crystallographically Characterized Five-Coordinate Iron Complexes Containing One or Two π Radical Ligands

type	complex	S_t^a	S_{Fe}^b	ref
I	$[\text{Fe}^{\text{II}}(\text{L})_2(\text{C}\equiv\text{NR})]$	0	1 or 0	this work
	$[\text{Fe}^{\text{II}}(\text{L})_2(\text{PR}_3)]$	0	1 or 0	this work
	$[\text{Fe}^{\text{II}}(\text{L}_{\text{N,S}})_2(\text{CN})]^-$	0	1 or 0	16
	$[\text{Fe}^{\text{II}}(\text{L}_{\text{N,S}})_2\{\text{P}(\text{OR})_3\}]$	0	1 or 0	16
II	$[\text{Fe}^{\text{III}}(\text{L})(\text{L})_2]$	0 (per dimer)	$3/2$	this work
	$[\text{Fe}^{\text{III}}(\text{L}_{\text{N,S}})(\text{L}_{\text{N,S}})_2]$	0 (per dimer)	$3/2$	16
	$[\text{Fe}^{\text{III}}(\text{L})(\text{L})(\text{PhCH-py})]$	1	$3/2$	this work
	$[\text{Fe}^{\text{III}}(\text{L}_{\text{S,S}})(\text{L}_{\text{S,S}})(\text{PR}_3)]$	1	$3/2$	17
III	$[\text{Fe}^{\text{III}}(\text{L})_2(\text{PR}_3)]^+$	$1/2$	$3/2$	this work
	$[\text{Fe}^{\text{III}}(\text{L})_2(\text{C}\equiv\text{NR})]^+$	$1/2$	$3/2$	this work
	$[\text{Fe}^{\text{III}}(\text{L})_2\text{I}]$	$1/2$	$3/2$	this work
	$[\text{Fe}^{\text{III}}(\text{L}_{\text{N,S}})_2\text{I}]$	$1/2$	$3/2$	16
	$[\text{Fe}^{\text{III}}(\text{L}_{\text{S,S}})_2(\text{PR}_3)]^+$	$1/2$	$3/2$	17
	$[\text{Fe}^{\text{III}}(\text{L}_{\text{N,O}})_2\text{I}]$	$1/2$	$3/2$	9, 10

^a Ground state of molecule. ^b Intrinsic spin state of the iron ion.

Table 6. X-Band EPR Spectra of Complexes Containing an $[\text{Fe}^{\text{III}}(\text{L}^{\text{ISQ}})_2\text{X}]$ ($S_t = 1/2$) Unit (Frozen Acetonitrile/Toluene 1:1 Mixture)

complex	g_{max}	g_{mid}	g_{min}	T, K
2^{ox}	2.276	2.085	2.009	10
3	2.2770	2.1168	2.0277	10
4^{ox}	2.131	2.069	2.018	27
5^{ox}	2.140	2.071	2.020	29
6	2.198	2.075	2.015	8

conjunction with magnetic Mössbauer spectra and showed that they are not consistent with the presence of low-spin ferric ions.¹⁶

The spectrum of **3** displayed in Figure 7 (bottom) exhibits an interesting, well-resolved hyperfine splitting pattern of nine lines at g_{min} . As we have shown before for similar spectra of $[\text{Fe}(\text{L}_{\text{N,O}}^{\text{ISQ}})_2\text{I}]$ ¹⁰ and $[\text{Fe}(\text{L}_{\text{N,S}}^{\text{ISQ}})_2\text{I}]$ ¹⁶ this hyperfine splitting cannot be due to hyperfine interactions to an ¹⁴N or ¹H nuclei because the central line is not split. It is a strong hyperfine interaction with the axial ¹²⁷I ($I = 5/2$, 100% natural abundance) which is affected by electric quadrupole interactions. A satisfactory fit was obtained by using the following parameters: (1) $g_{\text{max}} = 2.2770$, $g_{\text{mid}} = 2.1168$, $g_{\text{min}} = 2.0277$; (2) **A**-tensor components of which the first two are oriented along g_{max} and g_{mid} , $(3.0, 4.0, -16.0) \times 10^{-4} \text{ cm}^{-1}$ (they represent upper limits estimated from the envelope of the respective line); (3) the quadrupole coupling matrix (the sign of the main component is arbitrary), $P = (19.0, 15.0, 4.0) \times 10^{-4} \text{ cm}^{-1}$.

The unusual splitting and intensity pattern of the hyperfine lines owe their origin to large electric quadrupole interactions with the iodide ligand which mixes and shifts the m_I sublevels of the nuclear spin manifolds. This affects the transition probabilities and even induces “forbidden” transitions with virtually $\Delta m_I > 0$, particularly with a nonzero anisotropy factor η . Note that the influence of quadrupole interactions on EPR hyperfine patterns results from higher order effects. Reasonable simulations of the strong perturbations observed

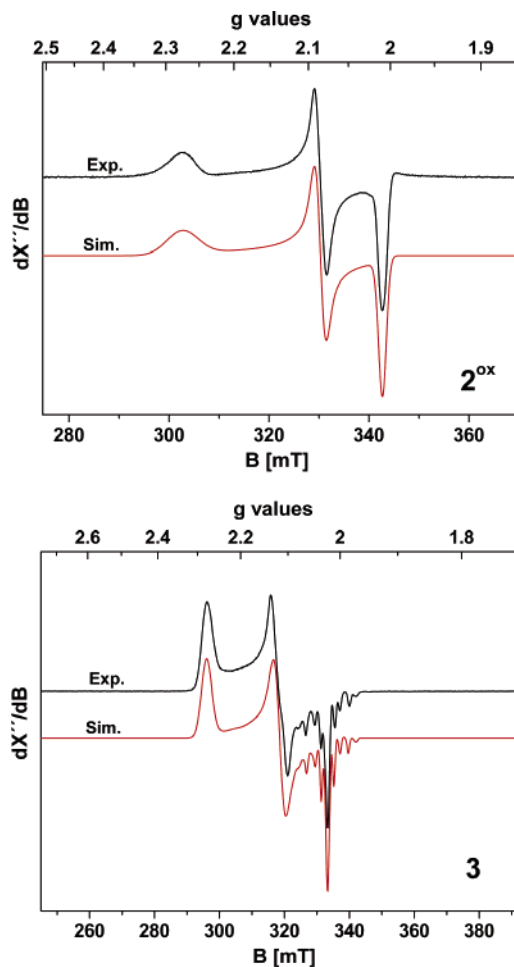


Figure 7. X-band EPR spectra of **2^{ox}** in frozen acetonitrile/toluene solution (1:1 v/v) at 10 K (top) (conditions: frequency 9.638 GHz; power 2.0 μW ; modulation 10 G) and **3** in frozen acetonitrile/toluene at 10 K (bottom) (conditions: frequency 9.439 GHz; power 10.1 μW ; modulation 5 G). For simulation parameters, see the text.

here require that the electric field gradient (EFG) tensor of iodine be oriented “off” from the principal axes system of the respective **A** tensor.

As we have shown previously,^{10,16} the EPR spectrum of **3** and corresponding magnetic Mössbauer spectra provide a direct spectroscopic indication for the presence of two ligand radicals $(\text{L}^{\text{ISQ}})^{\bullet-}$ and an intermediate-spin ferric in $S_{Fe} = 3/2$. The structure of the total spin ground-state $S_t = 1/2$ is then characterized by an antiferromagnetic alignment of the type $[\downarrow(S = 1/2), \uparrow(3/2), \downarrow(1/2)]$ which is due to a strong antiferromagnetic iron–ligand radical exchange interaction which dominates the inferior radical–radical interaction.

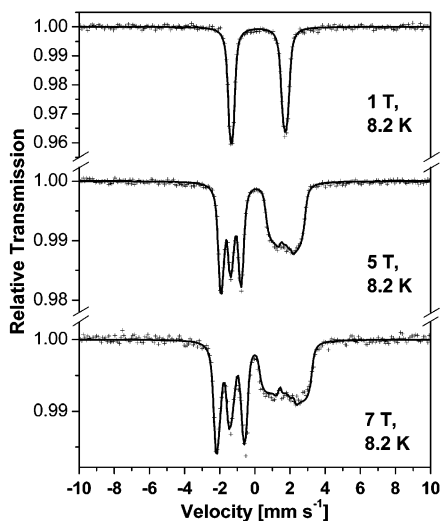
5. Mössbauer Spectroscopy. Zero-field Mössbauer spectra of polycrystalline samples were recorded at 80 K; the results are summarized in Table 7. The spectra of **1**, **2**, **2^{ox}**, and **3–7** consist of a single doublet with very similar isomer shift, δ , and quadrupole splitting, ΔE_Q , parameters: $\delta = 0.05\text{--}0.22 \text{ mm s}^{-1}$ and $\Delta E_Q = 2.26\text{--}3.06 \text{ mm s}^{-1}$.

The Mössbauer parameters for complex **1** are very similar to those reported for the dimeric, isomeric species $(\mu\text{-S,S})\text{-}[\text{Fe}^{\text{III}}(\text{L}_{\text{N,S}}^{\text{IP}})(\text{L}_{\text{N,S}}^{\text{ISQ}})]_2$ and $(\mu\text{-NH,NH})\text{-}[\text{Fe}^{\text{III}}(\text{L}_{\text{N,S}}^{\text{IP}})(\text{L}_{\text{N,S}}^{\text{ISQ}})]_2$, where $(\text{L}_{\text{N,S}}^{\text{IP}})^{2-}$ represents the 4,6-di-*tert*-butyl-2-iminothiophenolate dianion and $(\text{L}_{\text{N,S}}^{\text{ISQ}})^{\bullet-}$ is its one-electron-oxidized π

Table 7. Zero-Field Mössbauer Data of Complexes

complex	δ , mm s ⁻¹ ^a	$ \Delta E_Q $, mm s ⁻¹ ^b	Γ , mm s ⁻¹ ^c	T, K	S_{Fe}^d	S_t^e
1	0.22	2.68	0.36	80	$3/2$	0
2	0.13	2.96	0.36	80	0	0
2^{ox}	0.05	2.62	0.47	80	$3/2$	$1/2$
3	0.16	2.90	0.36	80	$3/2$	$1/2$
4	0.10	2.64	0.32	80	0	0
5	0.09	2.60	0.34	80	0	0
6	0.11	2.26	0.34	80	$3/2$	$1/2$
7	0.20	3.06	0.24	8.2	$3/2$	1

^a Isomer shift. ^b Quadrupole splitting. ^c Line width. ^d Intrinsic spin of the iron ion. ^e Spin ground state of complex.

**Figure 8.** Applied Mössbauer spectra of a solid sample of **7**.

radical monoanion: $\delta = 0.17$ and 0.20 mm s⁻¹, respectively; $\Delta E_Q = 2.73$ and 2.67 mm s⁻¹, respectively.¹⁶ This immediately implies that the [Fe^{III}(L^{ISQ})(L^{PDI})] chromophore possesses the same electronic structure as the previous two crystallographically characterized complexes with an [Fe^{III}(L^{IP}_{N,S})(L^{ISQ})] chromophore where a single π radical ligand is coupled antiferromagnetically to a central intermediate-spin ferric ion yielding an $S^* = 1$ state which in the dimers couple antiferromagnetically to the observed diamagnetic ground state.

The mononuclear paramagnetic complex **7** possesses an $S = 1$ ground state; the Mössbauer parameters are very similar to those reported for **1** which indicates the presence of the same [Fe^{III}(L^{ISQ})(L^{PDI})] chromophore with an intermediate-spin ferric ion ($S_{Fe} = 3/2$) coupled antiferromagnetically to a single π radical ligand ($S_{red} = 1/2$) yielding the observed triplet ground state in **7**.

Figure 8 displays magnetically perturbed Mössbauer spectra of **7** from the simulations using the following parameters from magnetic susceptibility measurements: $S_t = 1$; $D_t = +48$ cm⁻¹; $E/D = 0.2$; $g = 2.0$ (fixed). The parameters given in Table 8 have been derived. The magnetic hyperfine tensor is dominated by two negative “x” and “y” components and a very small positive or as in this case zero “z” component. By using spin projection techniques it is possible to convert the magnetic hyperfine tensor values $A/g_N\beta_N$ ($S_t = 1$) to the intrinsic values which are characteristic for the local spin state of the ferric ion ($S_{Fe} = 3/2$); see Table

8. The quadrupole tensor was found to be oriented off from the axes system of the **D** tensor by the following Euler angles: $\alpha = 108^\circ$; $\beta = 92^\circ$; $\gamma = 0^\circ$. These values agree nicely with those reported for other five-coordinate intermediate spin ferric ($S_{Fe} = 3/2$) complexes without π radical ligands ($S_t = 3/2$).^{17,18}

Similarly, the applied field Mössbauer spectra of **2^{ox}** ($S_t = 1/2$) and **3** ($S_t = 1/2$) indicate the presence of an intermediate-spin ferric ion and two ligand π radicals, respectively.

Complexes **2**, **4**, and **5** with a strong π acceptor ligand (phosphane or isocyanide) display isomer shifts in the narrow range 0.09 – 0.13 mm s⁻¹ and large quadrupole splittings in the range 2.60 – 2.94 mm s⁻¹. These mononuclear species are diamagnetic ($S_t = 0$). The data resemble closely those reported for diamagnetic [Fe^{II}(L^{ISQ})₂(CN)]⁻ and [Fe^{II}(L^{ISQ})₂(P(OPh)₃)] ($\delta = 0.05$ and 0.06 mm s⁻¹, respectively; $\Delta E_Q = 2.98$ and 2.92 mm s⁻¹).¹⁶ Interestingly, Scheidt et al.¹⁹ have reported similar Mössbauer parameters containing a redox-innocent porphinate and a nitrite ligand for the diamagnetic five-coordinate complex [Fe^{II}(TpivPP)(NO₂)]⁻ ($\delta = 0.41$ mm s⁻¹; $\Delta E_Q = 2.28$ mm s⁻¹ at 4.2 K). If the present complexes **2**, **4**, and **5** do in fact contain a low-spin ferrous ion (d^6 , $S_{Fe} = 0$), the spins of the two π radical ligands must be coupled strongly antiferromagnetically to enforce the observed $S = 0$ ground state.

A different model would assume the presence of an intermediate-spin ferrous ion ($S_{Fe} = 1$) which conceivably could be coupled antiferromagnetically to the two ligand radicals yielding the $S_t = 0$ ground state. This model would be in good agreement with the observed large quadrupole splitting. Four-coordinate porphinato and phthalocyanato complexes of Fe^{II} are known to possess an $S_t = 1$ ground state with large quadrupole splitting parameters of ~ 1.6 – 2.7 mm s⁻¹ and isomer shift values of ~ 0.5 mm s⁻¹.²⁰ Five-coordinate intermediate-spin ferrous complexes are also known²¹ as well as a few six-coordinate species.²²

Thus, at this point the Mössbauer spectra of diamagnetic complexes **2**, **4**, and **5** containing an [Fe^{II}(L^{ISQ})₂] chromophore do not allow us to distinguish between the two models presented above which invoke a diamagnetic low-spin ($S_{Fe} = 0$) or a paramagnetic intermediate-spin ($S_{Fe} = 1$) central ferrous ion.

Discussion

In this study we have identified three types of five-coordinate iron complexes containing two *o*-phenylenediamine-derived ligands in the equatorial positions of a square-

- (18) (a) Keutel, H.; Käpplinger, I.; Jäger, E.-G.; Grodzicki, M.; Schünemann, V.; Trautwein, A. X. *Inorg. Chem.* **1999**, *38*, 2320. (b) Kostka, K. L.; Fox, B. G.; Hendrich, M. P.; Collins, T. J.; Rickard, C. E. F.; Wright, L. J.; Münck, E. *J. Am. Chem. Soc.* **1993**, *115*, 6746.
 (19) Nasri, H.; Ellison, M. K.; Krebs, C.; Huynh, B. H.; Scheidt, W. R. *J. Am. Chem. Soc.* **2000**, *122*, 10795.
 (20) (a) Medhi, O. K.; Silver, J. *J. Chem. Soc., Chem. Commun.* **1989**, 1199. (b) Dale, B. W.; Williams, R. J. P.; Edwards, P. R.; Johnson, C. E. *J. Chem. Phys.* **1968**, *49*, 3445.
 (21) Bacci, M.; Ghilardi, C. A.; Orlandini, A. *Inorg. Chem.* **1984**, *23*, 2798.
 (22) Figg, D. C.; Herber, R. H.; Felner, I. *Inorg. Chem.* **1991**, *30*, 2535.

Table 8. Applied-Field Mössbauer Spectra of Five-Coordinate Complexes Containing an Intermediate Spin Ferric Ion ($S_{\text{Fe}} = 3/2$)

complex	T, K	$\delta, \text{mm s}^{-1}$	$\Delta E_Q, \text{mm s}^{-1}$	η	$A/g_N\beta_N(S_i), T$	$A/g_N\beta_N(S_{\text{Fe}} = 3/2), T$	S_i	S_{Fe}
2^{ox}	4.2	0.06	+2.82	0.0	-5.51	-3.31	$1/2$	$3/2$
					-22.76	-13.66		
3	4.2	0.15	+3.03	0.24	+0.67	+0.40	$1/2$	$3/2$
					-9.49	-5.69		
					-28.32	-16.99		
7	4.2	0.20	+3.06	0.50 ^c	+1.77	1.06	1	$3/2$
					-16.77	-13.42		
					-49.49	-39.59		
[Fe ^{III} [N ₄]] ^a	4.2	0.19	+3.56	0	0	0	$3/2$	$3/2$
[Fe ^{III} [S ₄](py)] ^{-b}	4.2	0.34	+2.94	0.02	-12.7	-12.7	$3/2$	$3/2$
					+0.5	+0.5		
					-19.13	-32.24		
						+1.54		

^a [N₄]²⁻ = 6,13-bis(ethoxycarbonyl)-5,14-dimethyl-1,4,8,11-tetraazacyclotetradeca-14,6,12,14-tetraenato dianion.¹⁷ ^b [S₄]⁴⁻ = bis(benzene-1,2-dithiolate); py = 4-*tert*-butylpyridine.¹⁶ ^c Euler angles: 108, 92, 0°.

based pyramidal coordination polyhedron and a monodentate ligand X (a π -acceptor, π -donor, or a simple σ -donor) in the apical position. These are the following: (1) complexes of type I containing the [Fe^{II}(L^{ISQ})₂] chromophore where the central ferrous ion possesses either an $S_{\text{Fe}} = 0$ or 1 intrinsic spin state which couples to two ligand radicals, (L^{ISQ})⁻, yielding the observed $S_i = 0$ ground state; (2) complexes of type II containing the [Fe^{III}(L^{ISQ})(L^{PDI})] chromophore with a central intermediate-spin ferric ion ($S_{\text{Fe}} = 3/2$) and a single π radical ligand ($S_{\text{rad}} = 1/2$) and a closed-shell, aromatic dianion (L^{PDI})²⁻ (the intrinsic spins S_{Fe} and S_{rad} couple strongly antiferromagnetically yielding an $S_i = 1$ state); (3) complexes of type III containing the [Fe^{III}(L^{ISQ})₂] chromophore where an intermediate-spin ferric ion ($S_{\text{Fe}} = 3/2$) couples antiferromagnetically with the $S_{\text{rad}} = 1/2$ spins of two π radical monoanions (L^{ISQ})⁻ affording an $S_i = 1/2$ ground state. In the following we identify the spectroscopic features of each of these three types.

1. [Fe^{II}(L^{ISQ})₂X] ($S_i = 0, S_{\text{Fe}} = 0$ or **1).** The type I [Fe^{II}(L^{ISQ})₂] chromophore in mononuclear, diamagnetic complexes **2**, **4**, and **5** is characterized by a single very intense absorption maximum at ~ 710 nm ($\epsilon \sim 2 \times 10^4 \text{ M}^{-1} \text{ cm}^{-1}$) which is tentatively assigned to a spin- and dipole-allowed ligand-to-ligand charge transfer (LLCT) band. This band has been analyzed in detail for the square planar complexes [M(L^{ISQ})₂] (M = Ni^{II}, Pd^{II}, Pt^{II}) in ref 2a,b.

It is remarkable that the same chromophore has been identified in [Fe^{II}(L^{ISQ})₂(P(OPh)₃)] and [Fe^{II}(L^{ISQ})₂(CN)]⁻, which display both a LLCT band at 690 (2.4×10^4) and 709 nm ($1.0 \times 10^4 \text{ M}^{-1} \text{ cm}^{-1}$), respectively.¹⁶ Their Mössbauer parameters are also very similar (at 80 K $\delta = 0.05$ and 0.06 mm s^{-1} ; $\Delta E_Q = 2.98$ and 2.92 mm s^{-1} , respectively); they are nearly the same as those for **2**, **4**, and **5** (Table 7).

From X-ray structure determinations of **2**, **5**, and [Fe^{II}(L^{ISQ})₂(P(OPh)₃)],¹⁵ the presence of two *o*-benzosemiquinonate(1-) π radicals in each complex has been clearly established rendering the oxidation state of the central iron ion +II. The intrinsic spin state at this ferrous ion, namely $S_{\text{Fe}} = 0$ or 1 (low or intermediate spin), remains unclear at this point. Spectroscopically both interpretations are conceiv-

able. Large quadrupole splittings would in principle favor an intermediate-spin description, but the low symmetry of the five-coordinate complexes with a single apical π -acceptor ligand would also be compatible with the data for an $S_{\text{Fe}} = 0$ species.¹⁹⁻²² The observed diamagnetic ground-state $S_i = 0$ of these five-coordinate species could result either from intramolecular antiferromagnetic (af) coupling between two ligand π radicals mediated by a low-spin ferrous ion or, alternatively, from an af coupling between an intermediate-spin ferrous ion and two π radicals.

The exact nature of this type I electronic structure is at present ambiguous. High-quality ab initio calculations are presently performed in our laboratory to resolve this interesting question. We note that a third possibility for the description of the electronic structure in diamagnetic type I complexes may exist: [Fe^{III}(L^{ISQ})(L^{PDI})] ($S_{\text{Fe}} = 1/2; S_i = 0$) with a central, low-spin ferric ion coupled antiferromagnetically to a single π radical monoanion (L^{ISQ})⁻. At present we discard this possibility because it does not provide a good model for the observed intense absorption at 700 nm. In addition, five-coordinate, low-spin ferric complexes are rather rare.

2. [Fe^{III}(L^{ISQ})(L^{PDI})X] ($S_i = 1; S_{\text{Fe}} = 3/2$). Complex **7** represents this type II class of complexes where X is a neutral, 4-substituted pyridine ligand. Its electronic spectrum (Figure 5, Table 4) exhibits a single very intense charge-transfer band at ~ 500 nm ($\epsilon \sim 10^4 \text{ M}^{-1} \text{ cm}^{-1}$) which we assign tentatively to a ligand-to-metal charge-transfer band (LMCT). The central five-coordinate ferric ion possesses an intrinsic intermediate spin ($S_{\text{Fe}} = 3/2$) as has been established by applied field Mössbauer spectroscopy (Table 8).

The dimeric complex **1** belongs to the same type II class. Two [Fe^{III}(L^{ISQ})(L^{PDI})] halves with $S^* = 1$ are probably bridged by the two electron-rich (L^{PDI})²⁻ ligands via two R-NH bridges yielding the observed $S_i = 0$ ground state.

As shown in Table 5, we have identified this type II electronic structure previously for the dimers (μ -S,S)[Fe^{III}(L^{ISQ})(L^{N,S})]₂ in ref 15 and for the mononuclear species [Fe^{III}(L^{ISQ})(L^{S,S})(PR₃)] ($S_i = 1; S_{\text{Fe}} = 3/2$) in ref 17. It is gratifying that the electronic spectra and Mössbauer param-

eters of these species resemble closely those reported here for **1** and **7**.

3. [$\text{Fe}^{\text{III}}(\text{L}^{\text{ISQ}})_2\text{X}$] ($S_t = 1/2$; $S_{\text{Fe}} = 3/2$). The type III class of compounds such as **2^{ox}**, **3**, **4^{ox}**, **5^{ox}**, and **6** all contain the [$\text{Fe}^{\text{III}}(\text{L}^{\text{ISQ}})_2$] chromophore with an $S_t = 1/2$ ground state. These five-coordinate species comprise two ligand π radicals (L^{ISQ}^-) and an intermediate-spin ferric ion ($S_{\text{Fe}} = 3/2$) as is clearly shown by the applied-field Mössbauer parameters. The X-ray structure determinations of **2^{ox}**, **3**, and **6** unambiguously show the presence of two ligand π radicals. As is shown in Figure 5 and Table 4, their electronic spectra are similar. Two quite intense absorptions at ~ 500 nm ($\sim 10^4$ $\text{M}^{-1} \text{cm}^{-1}$) and ~ 630 nm ($\sim 10^4$ $\text{M}^{-1} \text{cm}^{-1}$) are characteristic for this chromophore.

A number of other complexes containing this chromophore have been identified previously.^{9,10,16,17} The ligand π radicals are ($\text{L}_{\text{N,S}}^{\text{ISQ}}^-$), ($\text{L}_{\text{S,S}}^{\text{ISQ}}^-$), and ($\text{L}_{\text{N,O}}^{\text{ISQ}}^-$), respectively, as summarized in Table 5.^{9,10,16,17} Warren's paramagnetic complexes [$\text{Fe}^{\text{III}}\{\text{C}_6\text{H}_4(\text{NH}_2)_2\}_2\text{I}$] and [$\text{Fe}^{\text{III}}\{\text{C}_6\text{H}_4(\text{NH}_2)_2\}_2(\text{PPh}_3)](\text{PF}_6)$] are type III complexes since their electronic spectra quite similar to those reported here for **2^{ox}** and **3**, respectively. Interestingly, the chloro complex [$\text{Fe}^{\text{III}}(\text{L}_{\text{N,O}}^{\text{ISQ}})_2\text{Cl}$] possesses a quar-

ter ground state ($S_t = 3/2$) which is obtained via antiferromagnetic coupling of a high-spin ferric ion ($S_{\text{Fe}} = 5/2$) with two ligand π radicals.^{9,10} The corresponding bromo complex [$\text{Fe}^{\text{III}}(\text{L}_{\text{N,O}}^{\text{ISQ}})_2\text{Br}$] displays spin crossover behavior $S_t = 3/2 \leftrightarrow S_t = 1/2$. Here, the central ferric ion undergoes a temperature-dependent high-spin \leftrightarrow intermediate spin transition.^{9,10}

In no case has a low-spin ferric ion ($S_{\text{Fe}} = 1/2$) been identified in these type III complexes as has been suggested by Warren.⁶ As shown above, the applied-field Mössbauer and EPR spectra of these complexes rule out such a description.¹⁶

Acknowledgment. K.C. thanks the Max-Planck Society for a fellowship. We are grateful to the Fonds der Chemischen Industrie for financial support.

Supporting Information Available: Figure S1, displaying the temperature magnetic moments of complexes **2^{ox}**, **3**, and **6**, and X-ray crystallographic files for complexes **2**, **2^{ox}**, **3**·THF, **5**, **6**, **7**· $\text{C}_{16}\text{H}_{19}\text{N}$, and **8**. This material is available free of charge via the Internet at <http://pubs.acs.org>.

IC050829K